

PLANE WAVE PROPAGATION IN EXPONENTIALLY GRADED ISOTROPIC NON LOCAL GENERALIZED THERMOELASTIC SOLID MEDIUM UNDER INITIAL STRESS AND GRAVITY

K. Kumar^{1*}, S. Malik² and A. Antil²

¹Department of Mathematics, Deenbandhu Chhotu Ram University of Science and Technology, INDIA

²Department of Physical Science (Mathematics), Baba Mastnath University, INDIA

E-mail: dahiya_krishan@rediffmail.com

The work is concerned with the propagation of plane waves at the free half space in a exponentially graded isotropic nonlocal generalized thermoelastic solid medium under initial stress and gravity. We study the incidence of P or SV waves at the free half space. We found three reflected waves namely P , thermal T and SV waves propagating with different speeds. The phase speeds, reflection and energy coefficients are calculated in closed form to study the impact of gravity and initial stress parameter on reflection and energy coefficients. These are calculated numerically and shown graphically with the help of MATLAB. Some special cases of interest are also drawn from the present investigation.

Key words: thermoelasticity, non-local, initial stress, exponential graded.

1. Introduction

The stresses that are already existing in the structure and are not impacted by outside forces are known as initial stresses. The static and dynamic phenomena of elastic bodies are significantly impacted by initial strains. Several authors have examined how different waves propagate in different media that contain initial stresses. Biot [1] studied the influence of initial stress on elastic waves. He found that the law of propagation is unaffected by uniform hydrostatic pressure. In the year 1971, Edelen and Laws [2] developed the thermodynamics of systems with nonlocality. Nonlocal continuum mechanics was introduced by Edelen *et al.* [3], in the same year. Following these pioneer works, Eringen and Edelen [4] formulated nonlocal elasticity in 1972. Altan [5] proved uniqueness of initial boundary value problems in nonlocal elasticity. Othman and Song [6] discussed reflection of plane waves from an elastic solid half-spaces under hydrostatic initial stress without energy dissipation. The effect of the initial stresses on the reflection and transmission of plane quasi-vertical transverse waves in piezoelectric materials was presented by Abd-Alla and Alseikh [7]. Abd-Alla [8] studied propagation of Rayleigh waves in a rotating orthotropic material elastic half-space under initial stress and gravity. With the help of government equations and Lamé's potentials in a homogeneous, orthotropic elastic material, he derived the frequency equation and velocity for Rayleigh waves, taking into account rotation, initial stress and gravity field. Guo and Wei [9] obtained the effects of initial stress on the reflection and transmission waves at the interface between two piezoelectric half-spaces. Othman *et al.* [10] investigated the effect of rotation and initial stress on a generalised thermoelastic medium with two temperatures. Othman *et al.* [11] studied reflection of plane waves from a rotating magnetothermoelastic medium with two temperatures and initial stress under three theories. Das *et al.* [2019] showed how plane waves can be reflected off the stress-free, insulated isothermal borders of a nonlocal thermoelastic material. The wave propagation at the interface of two isolated half-spaces of thermoelastic media with initial stress was analysed by Tothhawang and Singh [12].

Poonam *et al.* [13] studied plane wave propagation in functionally graded isotropic couple stress thermoelastic solid media under initial stress and gravity. Again they investigated the impact that the initial stress

* To whom correspondence should be addressed

and gravity on the coefficients of refraction and reflection. Dey *et al.* [14] studied the problem of the effect of gravity and initial stress on the propagation of torsional surface waves in dry sandy medium. They investigated that the gravitational field will always permit the propagation of torsional waves, if the Whittaker function expands to a linear term. A quadratic-term extension of the Whittaker function suggests that the medium may include two such wave fronts. Regardless of whether the medium is dry sandy or elastic, it was determined that torsional surface waves can always propagate in the presence of a gravity field but cannot in a sandy media without it.

In general, we look at three different kinds of thermoelasticity theories that are found in the books: generalized, uncoupled and coupled. However, there are two problems with the conventional uncoupled theory of thermoelasticity that prevent it from being compatible with real-world experiments.

The first phenomenon is that there is no elastic term in this theory's energy equation and the second phenomenon states that thermal waves propagate at an infinite speed. Biot [15] removed the first shortcoming by introducing the theory of coupled thermoelasticity. Although he included connected governing equations, the theory still had the another flaw. The shortcoming corresponding to infinite speed of propagation in the uncoupled theory of thermoelasticity was investigated by several researchers, for example Szekeres [16], Ferkas and Szekeres [17] and Chandrasekharaiah [18]. Szekeres [16] explained that the Fourier law of heat conduction is the most effective model in physics in spite of that it has fundamental errors. These authors showed that altering the Fourier law of heat conduction leads to a hyperbolic differential equation with a finite propagation speed.

The first generalization to the theory of thermoelasticity was made by Lord and Shulman [19]. By adding a term flux rate to the traditional Fourier's law of heat conduction, they were able to create a wave-like heat equation. Green and Lindsay [20] gave the second generalization by introducing temperature rate among constitutive variables that includes two thermal relaxation times and does not violate the classical law of heat conduction when the body under consideration has a centre of symmetry. Later on more generalizations were developed by many reserearchers e.g. (Hetnarski and Ignaczak [21], Green and Naghdi theory [22], Tzau [23]).

Inan and Eringen [24] discussed longitudinal wave propagation in thermoelastic plates in the context of nonlocal elasticity and obtained field equations using integral form of constitutive equations, balance of momenta and energy. Eringen [25] discussed theories of nonlocal elasticity, fluid dynamics and electromagnetic field that included nonlocality in both space and time. Khurana and Tomar [26] investigated the five basic waves consisting of three longitudinal waves and two transverse waves propagating through an isotropic non-local microstretch solid of infinite extent with distinct speeds.

Kumar and Kumar [27] investigated reflection and transmission at a plane interface in a modified couple stress generalised thermoelastic solid half space and observed that amplitude ratios obtained due to incidence of a set of coupled longitudinal waves and coupled transverse waves are functions of the angle of incidence, frequency and are affected by the couple stress properties of media. Singh *et al.* [28] derived governing relations and equations for a nonlocal elastic solid with voids and investigated propagation of time harmonic plane waves in an infinite nonlocal elastic solid material with voids. Three fundamental waves two sets of interconnected longitudinal waves and one independent transverse wave have been shown to have varying rates of motion. The dispersion relation for the Rayleigh-type surface wave, which was discovered to be complicated in nature, was developed by Kaur *et al.* [29]. The Rayleigh-type wave was found to have a single mode that faces the same critical frequency as the shear wave. Additionally, it was demonstrated that the medium's voids and nonlocality cause dispersion. Sarkar and Tomar [30] investigated propagation of time harmonic plane waves in an infinite nonlocal thermoelastic solid having void pores and found there exist three sets of coupled dilatational waves and one independent transverse wave travelling with distinct speeds in the medium. While transverse waves are nonattenuating and coupled dilatational waves are attenuating. They observed that these waves are dispersive in character and controlled by a nonlocal parameter.

Poonam *et al.* [31] presented wave propagation in nonlocal couple stress thermoelastic solid. Pramanik and Biswas [32] developed a new model of non-local thermoelasticity with energy dissipation and presented graphically the phase velocity, attenuation coefficients, specific loss with respect to frequency. Poonam *et al.* [33] investigated the fundamental solution in a non-local couple stress micropolar thermoelastic solid with voids and observed that the non-local and void parameter had a great effect on the penetration depth, specific loss and attenuation coefficients. Gupta *et al.* [34] investigated reflection and transmission in non-local couple stress micropolar thermoelastic media. They calculated amplitude ratios of reflection and refraction

phenomenon numerically and presented them graphically. Ali *et al.* [36] analyzed hall current effects and fractional order nonlocal theory on plane wave reflection in a rotating isotropic medium. Bibi *et al.* [37] investigated propagation and reflection of thermoelastic wave in a rotating nonlocal fractional order porous medium under hall current influence. Azhar *et al.* [38-39] found influence of hall current on thermoelastic wave behaviour in viscoelastic fractional-order rotating porous solids and investigated reflection phenomenon of plane waves in a fractional order thermoelastic rotating medium using nonlocal theory. Bibi and Ali [40] discussed reflection and transmission phenomenon of plane waves at the interface of diffusive viscoelastic porous rotating isotropic medium under hall current and nonlocal thermoelastic porous solid.

In the present paper, we formulate a mathematical model for a linear homogeneous isotropic non-local generalized thermoelastic solid under initial stresses and gravity. After formulation, the material constants presented exponentially graded with respect to depth and reflection coefficients for incident P and SV waves are obtained numerically and presented graphically under the influence of initial stresses and gravity simultaneously.

2. Mathematical formulation

The plane interface coincide with xz – plane in the co-ordinate system $Oxyz$ and z axis is taken downward into the medium and the interface is taken along $z = 0$ as shown in Fig.[1].

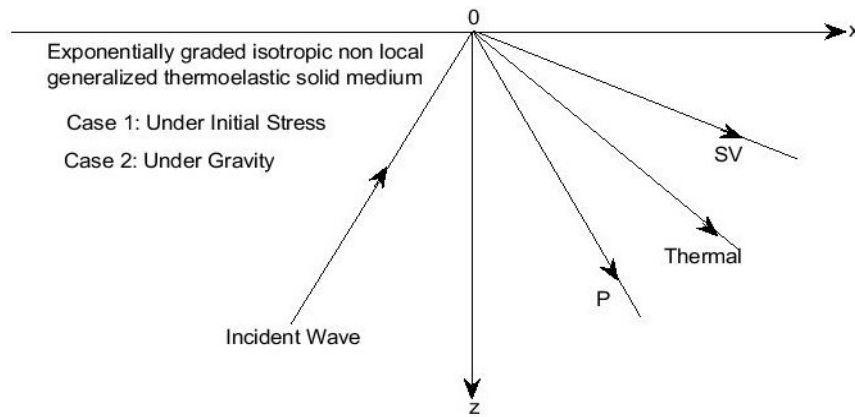


Fig.1. Geometry of the problem.

Following Biot [15], Lord and Shulman [19], Eringen [24] and Balta and Suhubi [35] theories, the stress–strain relation involving hydrostatic pressure h for a linear, homogeneous, isotropic and nonlocal generalized thermoelastic solid are written as

$$t_{xx} = (\lambda + 2\mu + h) \frac{\partial u}{\partial x} + (\lambda + h) \frac{\partial w}{\partial z} - \gamma T, \quad (2.1)$$

$$t_{zz} = (\lambda + 2\mu + h) \frac{\partial w}{\partial z} + (\lambda + h) \frac{\partial u}{\partial x} - \gamma T, \quad (2.2)$$

$$t_{xz} = (\mu + h) \left(\frac{\partial u}{\partial z} + \frac{\partial w}{\partial x} \right) \quad (2.3)$$

and the heat conduction equation is given by

$$K \nabla^2 T = \left(1 + \tau \frac{\partial}{\partial t} \right) \left[\rho C_e \left(1 - \epsilon^2 \nabla^2 \right) \frac{\partial}{\partial t} + \gamma T_0 \left(\frac{\partial}{\partial t} \left(\frac{\partial u}{\partial x} + \frac{\partial w}{\partial z} \right) \right) \right]. \quad (2.4)$$

3. Dynamics of exponentially gradient couple stress thermoelastic medium M

We denote $\lambda^{(l)}$, $\mu^{(l)}$ and $\gamma^{(l)}$ are elastic constants, h_l and ρ_l denote pressure and density resp. in media M of the structure. The material constants that are shown as an exponential function with respect to depth are

$$\begin{aligned}\lambda^{(l)} &= \bar{\lambda} e^{\beta_l x}, \quad \mu^{(l)} = \bar{\mu} e^{\beta_l x}, \quad \gamma^{(l)} = \bar{\gamma} e^{\beta_l x}, \\ \rho_l &= \bar{\rho} e^{\beta_l x}, \quad h_l = \bar{h} e^{\beta_l x}, \quad K^{(l)} = \bar{K} e^{\beta_l x}\end{aligned}\quad (3.1)$$

where $\bar{\beta}$, \bar{K} and $\bar{\lambda}$, $\bar{\mu}$, \bar{a} are thermal and elastic constants resp. w.r.t. medium M . Pressure is represented by $h^{(l)}$, density by $\rho^{(l)}$ and gradient parameter by β_l . Now, we will talk about two distinct scenarios as

3.1. Case 1: When the couple stress thermoelastic media M are in the presence of initial stresses

Let $I_{xx}^{(l)}$ and $I_{zz}^{(l)}$ be the initial stresses in medium M along x and z -axis respectively, with the unknown exponentially gradient property. We have

$$I_{xx}^{(l)} = I_{22}^{(0s)} e^{\beta_l x}, \quad I_{zz}^{(l)} = I_{33}^{(0l)} e^{\beta_l x} \quad (3.2)$$

where the initial stresses $I_{xx}^{(l)}$ and $I_{zz}^{(l)}$ take the values $I_{xx}^{(0l)}$ and $I_{zz}^{(0l)}$ at the free surface.

The equations of motion for the couple stress thermoelastic solid media with the exponentially graded medium and initial stresses $I_{xx}^{(l)}$ and $I_{zz}^{(l)}$ acting along x and z -directions respectively, are (Biot [15])

$$\frac{\partial t_{xx}}{\partial x} + \frac{\partial t_{xz}}{\partial z} - I^{(l)} \frac{\partial \omega_{zx}}{\partial z} = \rho_l (l - \epsilon^2 \nabla^2) \frac{\partial^2 u}{\partial t^2}, \quad (3.3)$$

$$\frac{\partial t_{xz}}{\partial x} + \frac{\partial t_{zz}}{\partial z} - I^{(l)} \frac{\partial \omega_{zx}}{\partial x} = \rho_l (l - \epsilon^2 \nabla^2) \frac{\partial^2 w}{\partial t^2}, \quad (3.4)$$

where $I^{(l)} = I_z^{(l)} - I_x^{(l)}$ and $\omega_{zx} = \frac{1}{2} \left(\frac{\partial w}{\partial x} - \frac{\partial u}{\partial z} \right)$.

Using Eq.(3.2), we obtain

$$I^{(l)} = P^{(l)} e^{\beta_l x} \text{ with } P^{(l)} = I_x^{(0l)} - I_z^{(0l)}.$$

We present the displacement potentials ϕ and ψ in accordance with the Helmholtz decomposition theorem on vectors as

$$u = \left(\frac{\partial \phi}{\partial x} - \frac{\partial \psi}{\partial z} \right), \quad w = \left(\frac{\partial \phi}{\partial z} + \frac{\partial \psi}{\partial x} \right). \quad (3.5)$$

On solving Eq.(2.4) and (3.1)-(3.5), we obtain

$$(\bar{\lambda} + 2\bar{\mu} + \bar{h})\nabla^2\phi = \rho_I(l - \epsilon^2\nabla^2)\frac{\partial^2\phi}{\partial t^2} + \bar{\gamma}T, \quad (3.6)$$

$$I^{(l)}\nabla^2\psi = \rho_I(l - \epsilon^2\nabla^2)\frac{\partial^2\psi}{\partial t^2}, \quad (3.7)$$

$$\bar{K}\nabla^2T = \left(\frac{\partial}{\partial t} + \tau\frac{\partial^2}{\partial t^2}\right)\left[\rho_II C_e(l - \epsilon^2\nabla^2)T + T_0\bar{\gamma}\nabla^2\phi\right]. \quad (3.8)$$

According to Ottman *et al.* [6], the plane wave propagation for Eqs (3.6)-(3.8) in an isotropic nonlocal generalized thermoelastic solid is determined by

$$\{\phi, \psi, T\} = \{\phi_I, \psi_I, T_I\} \exp i l (x \sin \theta_0 + z \cos \theta_0) \quad (3.9)$$

where ι denote iota, ϕ_I, ψ_I, T_I are scalars, S and l denote velocity and wave number resp., $(\sin \theta, \cos \theta)$ is the projection of normal wave into xz -plane.

Using Eq.(3.9) in Eqs (3.6) and (3.8) and after simplification, yields a quadric equation as

$$S^2 + AS + B = 0 \quad (3.10)$$

where $S = \rho_I S$, $A = -(d_I + d_3 + \bar{\gamma}d_2)$, $B = d_I d_3$, $d_I = (\bar{\lambda} + 2\bar{\mu} + \bar{h}) - \rho_I \epsilon^2 \nabla^2$,

$$d_2 = \frac{\bar{\gamma}T_0}{\rho_I C_e}, \quad d_3 = \frac{\bar{K}}{C_e \tau^*} - \rho_I \epsilon^2 \nabla^2, \quad \tau^* = \tau + \iota \omega^{-l}, \quad \omega = \bar{K}S.$$

The roots of Eq.(3.10) are given by

$$S_{I,2}^2 = \frac{-A \pm \sqrt{A^2 - 4B}}{2}.$$

S_I and S_2 represent speeds of P and T -waves respectively.

The roots of Eq.(3.7) are given by

$$S_3^2 = \frac{\sqrt{I^{(l)2} - \rho_I \epsilon^2 \omega^2}}{\rho_I}.$$

The SV wave exists under the following condition

$$\epsilon^2 \omega^2 \leq \frac{I^{(l)}}{\rho_I}.$$

3.1.1. Reflection phenomenon

Incident P or SV at a thermally insulated or isothermal traction-free surface $z=0$ result into three reflected waves as P , thermal and SV waves as depicted in Fig.1. The potentials functions ϕ , T and ψ are written as linear combinations of solutions of incident and reflected waves as

$$\phi = N_0 \exp\{l_l(x \sin \theta_0 - z \cos \theta_0) - i\omega t\} + \sum_{i=1}^2 N_i \exp\{l_i(x \sin \theta_i + z \cos \theta_i) - i\omega t\}, \quad (3.11)$$

$$\psi = M_0 \exp\{l_3(x \sin \theta_3 + z \cos \theta_3) - i\omega t\} + M_l \exp\{l_3(x \sin \theta_3 + z \cos \theta_3) - i\omega t\}, \quad (3.12)$$

$$T = \vartheta_l N_0 \exp\{l_l(x \sin \theta_0 - z \cos \theta_0) - i\omega t\} + \sum_{i=1}^2 \vartheta_i N_i \exp\{l_i(x \sin \theta_i + z \cos \theta_i) - i\omega t\}. \quad (3.13)$$

N_0 and M_0 are the amplitudes of incident P and SV waves respectively and N_l , N_2 and M_l are the amplitudes of reflected P , thermal T and SV waves respectively. The coupling coefficients ϑ_i ($i = l, 2$) are obtained by using Eq.(3.11)-(3.13) in Eq.(3.6) as

$$\vartheta_i = \frac{l_j^2 (\rho_l Q_j^2 - d_l)}{\bar{\gamma}}.$$

3.1.2. Boundary conditions

At the interface $z=0$, the stress and temperature free boundary conditions are

$$t_{xx} = 0, \quad t_{xz} = 0, \quad T = 0. \quad (3.14)$$

The potentials given in Eq.(3.11)-(3.13) satisfy the boundary conditions Eq.(3.14) if the following relations hold at $z=0$

$$l^* \sin \theta_0 = l_l \sin \theta_l = l_2 \sin \theta_2 = l_3 \sin \theta_3, \quad l_l S_l = l_2 S_2 = l_3 S_3$$

where for incident P wave $l^* = l_l$ and for incident SV wave $l^* = l_3$. Using the potentials given in Eqs (3.11)-(3.13) in boundary conditions Eq.(3.14), we obtain a non-homogeneous system of three equations as

$$\sum_{j=1}^3 a_{ij} Z_j = b_i \quad (i = l, 2, 3) \quad (3.15)$$

where the amplitude ratios $Z_j = A_j / A_0$, $j = l, 2$ and $Z_3 = B_l / B_0$ are reflection coefficients of reflected P , thermal and SV waves, respectively. All non-zero entries of the matrix for P or thermal wave are defined as

$$a_{1l} = l, \quad a_{12} = \left[(\bar{\lambda} + \bar{h}) + 2\bar{\mu} (l - s_{2l}^2) \sin^2 \theta_0 + \frac{\bar{\gamma} \vartheta_2}{l_2^2} \right] / D_l s_{2l}^2,$$

$$a_{13} = 2\bar{\mu} \sin \theta_0 \sqrt{l - s_{3l}^2 \sin^2 \theta_0} / D_l s_{3l}, \quad a_{2l} = \sin \theta_0,$$

$$a_{22} = \sin 2\theta_0 \left[\sin \theta_0 + \sqrt{I - s_{2I}^2 \sin^2 \theta_0} \right] / s_{2I}^3, \quad a_{3I} = I, \quad a_{32} = \frac{\vartheta_2}{\vartheta_I}, \quad a_{33} = 0,$$

$$a_{23} = -\sin 2\theta_0 \left[\sin \theta_0 + \sqrt{I - s_{3I}^2 \sin^2 \theta_0} \right] / s_{3I}^3, \quad b_I = -I, \quad b_2 = -\sin 2\theta_0, \quad b_3 = I$$

where

$$s_{pI} = \frac{S_p}{S_I} \quad (p = 2, 3); \quad D_I = \left[(\bar{\lambda} + \bar{h}) + 2\bar{\mu} \sin^2 \theta_2 l_I^2 + \frac{\bar{\gamma} \vartheta_I}{l_I^2} \right]$$

The Energy coefficients for P wave are given by

$$E_1 = Z_I^2, \quad E_2 = \frac{(\bar{\lambda} + 2\bar{\mu} + \bar{h}) - \bar{\gamma} \vartheta_2 / l_2^2 \left(\frac{l_2}{l_I} \right)^3 \left(\frac{\cos \theta_2}{\cos \theta_I} \right)}{(\bar{\lambda} + 2\bar{\mu} + \bar{h}) - \bar{\gamma} \vartheta_I / l_I^2 \left(\frac{l_I}{l_I} \right)^3 \left(\frac{\cos \theta_I}{\cos \theta_I} \right)} Z_2^2$$

$$E_3 = \frac{\bar{\mu} \sin 2\theta_0 / l_3^2 \left(\frac{l_3}{l_I} \right)^3 \left(\frac{\cos \theta_3}{\cos \theta_I} \right)}{(\bar{\lambda} + 2\bar{\mu} + \bar{h}) - \bar{\gamma} \vartheta_I / l_I^2 \left(\frac{l_I}{l_I} \right)^3 \left(\frac{\cos \theta_I}{\cos \theta_I} \right)} Z_3^2$$

All non-zero entries of the matrix and the Energy coefficients for SV waves are given by

$$a_{1I} = \left[(\bar{\lambda} + \bar{h}) + 2\bar{\mu} (I - s_{I3}^2) \sin^2 \theta_0 + \frac{\bar{\gamma} \vartheta_I}{l_I^2} \right] / D_2 s_{I3}^2,$$

$$a_{I2} = \left[(\bar{\lambda} + \bar{h}) + 2\bar{\mu} (I - s_{23}^2) \sin^2 \theta_2 + \frac{\bar{\gamma} \vartheta_2}{l_2^2} \right] / D_2 s_{23}^2, \quad a_{I3} = I,$$

$$a_{2I} = \sin \theta_0 + \sqrt{I - s_{I3}^2 \sin^2 \theta_0} / s_{I3}^3, \quad a_{22} = \sin 2\theta_0 \left[\sin \theta_0 + \sqrt{I - s_{23}^2 \sin^2 \theta_0} \right] / s_{23}^3,$$

$$a_{23} = -\sin 2\theta_0, \quad a_{3I} = I, \quad a_{32} = \frac{\vartheta_2}{\vartheta_I}, \quad a_{33} = 0, \quad b_I = -I, \quad b_2 = -\sin 2\theta_0, \quad b_3 = I$$

where

$$s_{p3} = \frac{S_p}{S_3} \quad (p = I, 2); \quad D_2 = 2\bar{\mu} \sin \theta_0 \cos \theta_0.$$

$$E_1 = \frac{(\bar{\lambda} + 2\bar{\mu} + \bar{h}) - \bar{\gamma} \vartheta_I / l_I^2 \left(\frac{l_I}{l_3} \right)^3 \left(\frac{\cos \theta_I}{\cos \theta_3} \right)}{\bar{\mu}} Z_I^2,$$

$$E_2 = \frac{(\bar{\lambda} + 2\bar{\mu} + \bar{h}) - \bar{\gamma} \vartheta_2 / l_2^2 \left(\frac{l_2}{l_3} \right)^3 \left(\frac{\cos \theta_2}{\cos \theta_3} \right)}{\bar{\mu}} Z_2^2, \quad E_3 = Z_3^2.$$

3.2. Case 2: When the couple stress thermoelastic media M are in the presence of gravity

The initial stresses $I_{xx} = I_{zz} = -\rho_I g x$ are obtained due to the impact of gravity. Following Biot [15], the equations of motion are

$$\frac{\partial}{\partial x}(t_{xx} + \rho_I g u) + \frac{\partial t_{23}}{\partial z} = \rho_I (l - \epsilon^2 \nabla^2) \frac{\partial^2 u}{\partial t^2}, \quad (3.16)$$

$$\frac{\partial t_{23}}{\partial z} + \frac{\partial}{\partial z}(t_{zz} + \rho_I g u) = \rho_I (l - \epsilon^2 \nabla^2) \frac{\partial^2 w}{\partial t^2}. \quad (3.17)$$

The heat conduction equation is

$$\bar{K} \nabla^2 T = \left(\frac{\partial}{\partial t} + \tau \frac{\partial^2}{\partial t^2} \right) \left[\rho_I C_e (l - \epsilon^2 \nabla^2) T + T_0 \bar{\gamma} \nabla^2 \phi \right]. \quad (3.18)$$

By applying Eqs (3.16)-(3.18) to Eqs (2.1)-(2.4), (3.1), (3.5) and (3.9), we found the dynamical equations of motion for the propagation of plane waves in an exponentially graded medium M under the influence of gravity. These equations are identical to those we got for medium M in the presence of initial stress, with the exception of

$$\rho_I g \nabla^2 \psi = \rho_I (l - \epsilon^2 \nabla^2) g \frac{\partial^2 \psi}{\partial t^2} \quad (3.19)$$

We see that, the phase speed values S_s ($s = 1, 2$) for the set of coupled longitudinal waves are identical to those which we found when initial stress was present.

Substituting Eq.(3.9) in Eq.(3.19), we get

$$S_v^2 = \frac{\sqrt{\rho_I^2 g^2 - \rho_I \epsilon^2 \omega^2}}{\rho_I} \quad (3.20)$$

this corresponds to the SV wave's phase speed for medium M when gravity is present.

3.2.1 Boundary conditions

The boundary conditions provided by medium M in this instance are identical to those found in Eq.(3.14). Following the same procedure as previously described for initial stress, we obtain a matrix matching Eq.(3.15). The modified values of matrix a_{ij} for P or thermal wave are provided as

$$a_{11} = l, \quad a_{12} = \left[(\bar{\lambda} + \bar{h}) + 2\bar{\mu} (l - s_{2l}^2) \sin^2 \theta_0 + \frac{\bar{\gamma} \theta_2}{l_2'} \right] / D_l s_{2l}^2,$$

$$a_{13} = 2\bar{\mu} \sin \theta_0 \sqrt{l - s_{vl}^2 \sin^2 \theta_0} / D_l s_{vl}, \quad a_{21} = \sin \theta_0,$$

$$a_{22} = \sin 2\theta_0 \left[\sin \theta_0 + \sqrt{I - s_{2I}^2 \sin^2 \theta_0} \right] / s_{2I}^3, \quad a_{3I} = I, \quad a_{32} = \frac{\vartheta_2}{\vartheta_I}, \quad a_{33} = 0,$$

$$a_{23} = -\sin 2\theta_0 \left[\sin \theta_0 + \sqrt{I - s_{vI}^2 \sin^2 \theta_0} \right] / s_{vI}^3, \quad b_I = -I, \quad b_2 = -\sin 2\theta_0, \quad b_3 = I$$

where

$$s_{pI} = \frac{S_p}{S_I} \quad (p = 2, v); \quad D_I = \left[(\bar{\lambda} + \bar{h}) + 2\bar{\mu} \sin^2 \theta_2 l_I^2 + \frac{\bar{\gamma} \vartheta_I}{l_I^2} \right]$$

The Energy coefficients for P wave under gravity remains same as they are under initial stress. The modified values of matrix a_{ij} for SV wave are given as

$$a_{I1} = \left[(\bar{\lambda} + \bar{h}) + 2\bar{\mu} (I - s_{Iv}^2) \sin^2 \theta_0 + \frac{\bar{\gamma} \vartheta_I}{l_I^2} \right] / D_2 s_{Iv}^2,$$

$$a_{I2} = \left[(\bar{\lambda} + \bar{h}) + 2\bar{\mu} (I - s_{2v}^2) \sin^2 \theta_2 + \frac{\bar{\gamma} \vartheta_2}{l_2^2} \right] / D_2 s_{2v}^2, \quad a_{I3} = I,$$

$$a_{2I} = \left[\sin \theta_0 + \sqrt{I - s_{Iv}^2 \sin^2 \theta_0} \right] / s_{Iv}^3, \quad a_{22} = \sin 2\theta_0 \left[\sin \theta_0 + \sqrt{I - s_{2v}^2 \sin^2 \theta_0} \right] / s_{23}^3,$$

$$a_{23} = -\sin 2\theta_0, \quad a_{3I} = I, \quad a_{32} = \frac{\vartheta_2}{\vartheta_I}, \quad a_{33} = 0, \quad b_I = -I, \quad b_2 = -\sin 2\theta_0, \quad b_3 = I$$

where

$$s_{pv} = \frac{S_p}{S_v} \quad (p = I, 2); \quad D_2 = 2\bar{\mu} \sin \theta_0 \cos \theta_0.$$

The Energy coefficients for SV wave under gravity remains same as they are under initial stress.

4. Numerical analysis

The following aluminum metal physical constants are used in a numerical study taken from Singh and Bijarnia [41] to understand the impact of gravity and the initial stress parameter on the reflection and energy coefficients of reflected waves

$$\bar{\lambda} = 5.775 \times 10^{11} \text{ N / m}^2, \quad \bar{\mu} = 2.646 \times 10^{11} \text{ N / m}^2, \quad T_0 = 27^\circ \text{ C},$$

$$\bar{\gamma} = 7.04 \times 10^6 \text{ N / m}^2, \quad \rho_I = 2.7 \times 10^3 \text{ kg / m}^3, \quad \tau = 0.05 \times 10^{-11} \text{ s},$$

$$\bar{K} = 0.492 \times 10^2 \text{ W / mdegree}, \quad C_e = 0.236 \times 10^2 \text{ N / mdegree}, \quad \omega = 0.50, \quad \epsilon = 0.39.$$

The remaining variables that are considered are

$$\frac{I^{(l)}}{\bar{\mu}} = 0.2, 0.4, 0.6; \quad \frac{\rho_l g}{2\bar{\mu}} = 0.2, 0.4, 0.6.$$

The simple line, line having stars on it and dotted line correspond to the various values of initial stress which are equal to 0.2, 0.4 and 0.6.

4.1. Impact of initial stress of medium M on reflection and energy coefficient for P and SV waves

In this section, we discuss the effect of initial stress on variation of amplitude ratios Z_1, Z_2 and Z_3 and energy coefficients E_1, E_2 and E_3 with respect to incident angle θ_0 for P and SV waves respectively. Figures 2, 3 and 4 illustrate the impact of initial stress for longitudinal (P) wave on the reflection coefficients for different values of initial stress w.r.t. angle of incidence θ_0 . From Fig.2, it is observed that the behaviour of amplitude ratio Z_1 is similar for all values of initial stress. The value of Z_1 increases as θ_0 increases and takes maximum values at $\theta_0 = 45^\circ$ and decrease thereafter. Figure 3 illustrates that the value of amplitude ratio Z_2 decreases first for all the cases, becomes 0 at $\theta = 45^\circ$ and increase thereafter. It is noticed that the value of Z_2 decrease more sharply for initial stress having value 0.6 in comparison to other two values. Figure 4 shows that the value of Z_3 decreases sharply for $0^\circ \leq \theta_0 \leq 8^\circ$ and becomes almost 0 thereafter for all the three values of initial stress.

Figures 5, 6 and 7 represent the variation of energy coefficients E_1, E_2 and E_3 for different values of initial stress under consideration. Figure 5 presents that E_1 increase smoothly for smaller values of θ_0 , increase sharply up to middle range and then decrease for higher values of angle of incident. From Fig.6, it is noticed that value of energy coefficient E_2 decreases sharply for $0^\circ \leq \theta_0 \leq 30^\circ$ approximately, remains constant for middle values and increases sharply as angle of incident θ_0 increases. The behaviour of energy coefficient E_2 is similar for all the values of initial stress. Value of E_3 decreases sharply for small values of angle of incident and becomes 0 thereafter for all the values of initial stress under consideration.

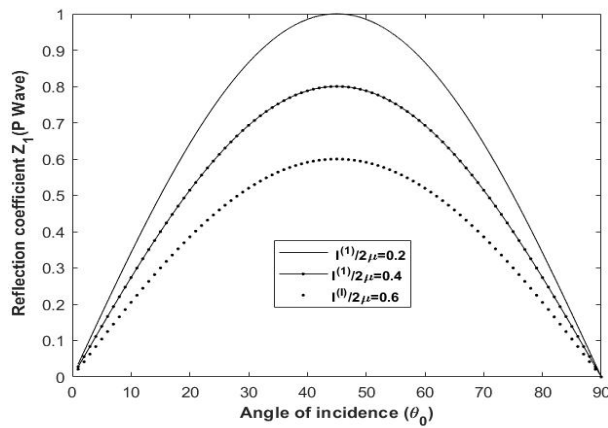


Fig.2. Impact of initial stress of M for P -wave on Reflection coefficient Z_1 versus θ_0 .

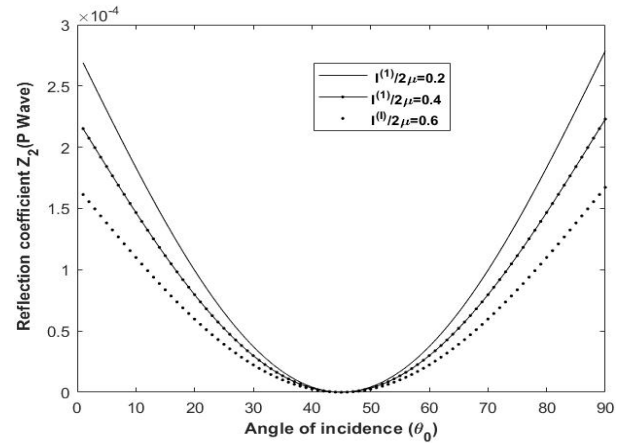


Fig.3. Impact of initial stress of M for P -wave on Reflection coefficient Z_2 versus θ_0 .

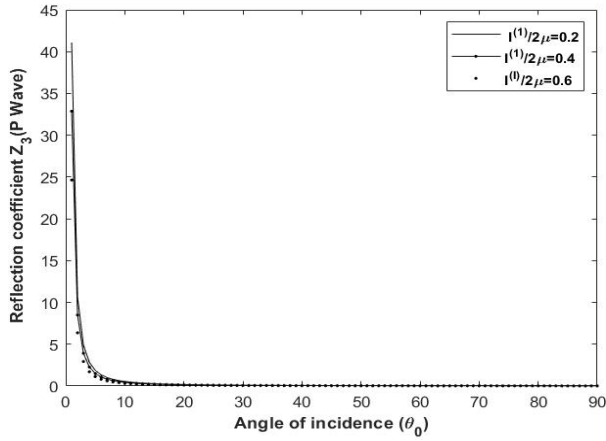


Fig.4. Impact of initial stress of M for P -wave on Reflection coefficient Z_3 versus θ_0 .

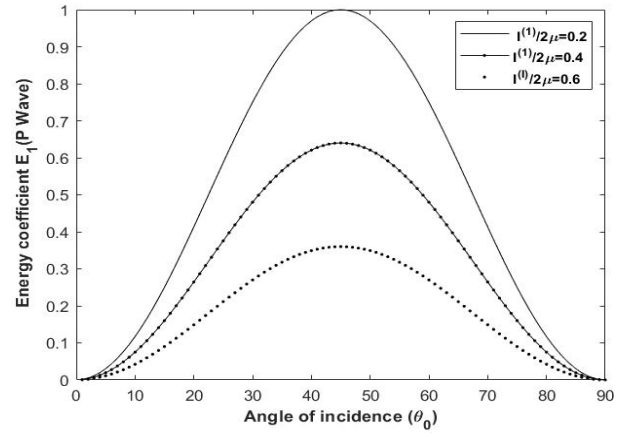


Fig.5. Impact of initial stress of M for P -wave on Energy coefficient E_1 versus θ_0 .

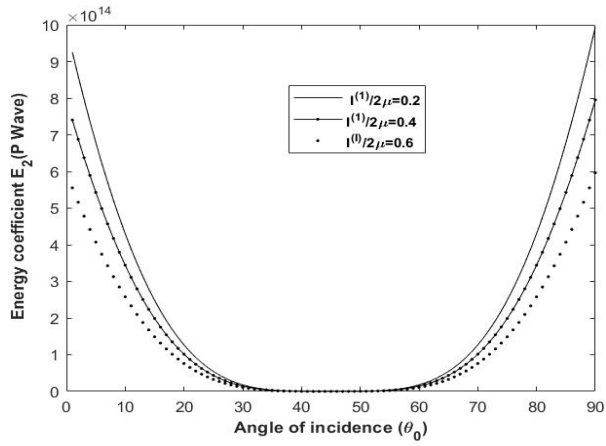


Fig.6. Impact of initial stress of M for P -wave on Energy coefficient E_2 versus θ_0 .

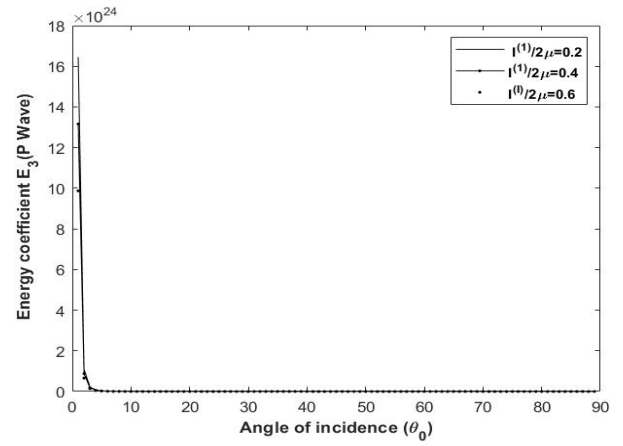


Fig.7. Impact of initial stress of M for P -wave on Energy coefficient E_3 versus θ_0 .

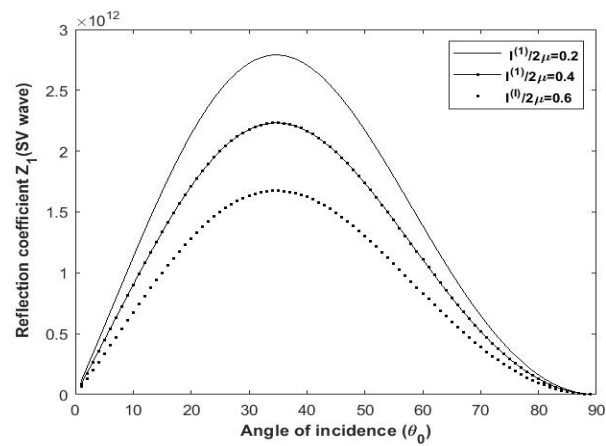


Fig.8. Impact of initial stress of M for SV -wave on Reflection coefficient Z_1 versus θ_0 .

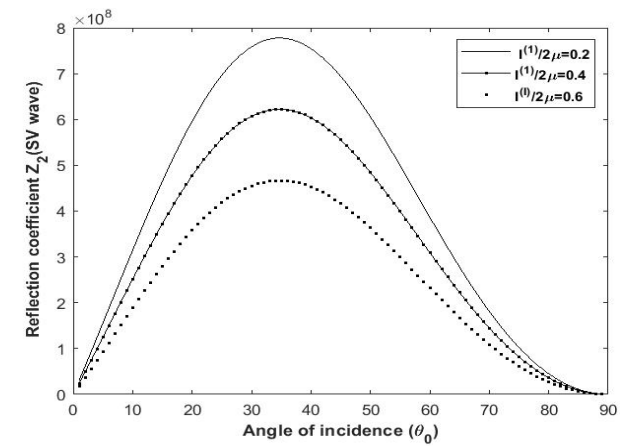


Fig.9. Impact of initial stress of M for SV -wave on Reflection coefficient Z_2 versus θ_0 .

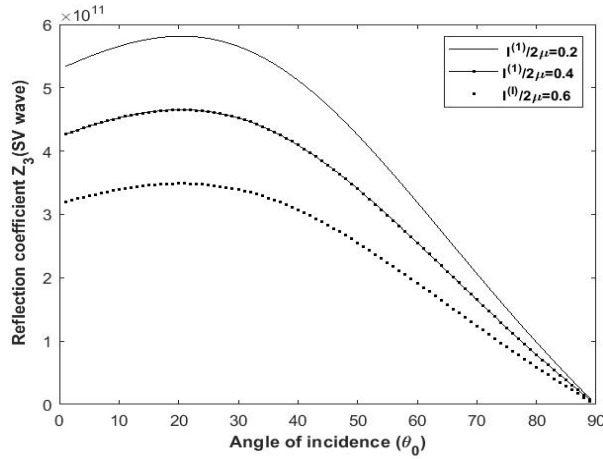


Fig.10. Impact of initial stress of M for SV -wave on Reflection coefficient Z_3 versus θ_0 .

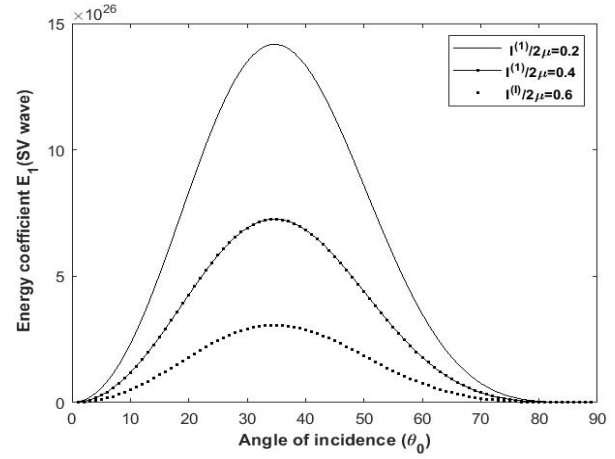


Fig.11. Impact of initial stress of M for SV -wave on Energy coefficient E_1 versus θ_0 .

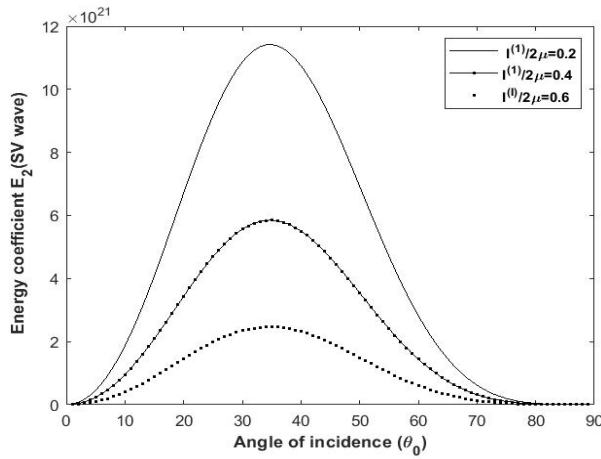


Fig.12. Impact of initial stress of M for SV -wave on Energy coefficient E_2 versus θ_0 .

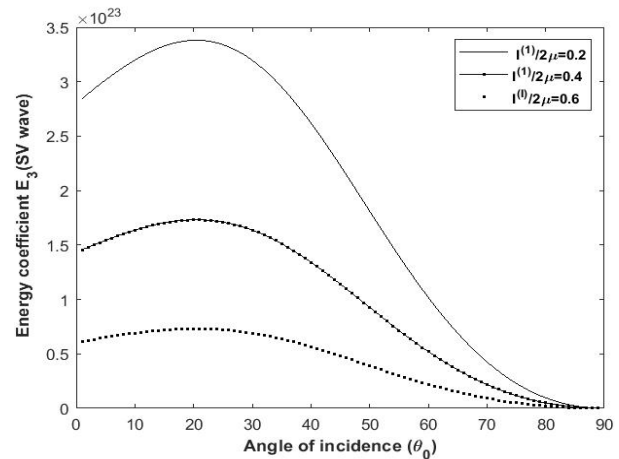


Fig.13. Impact of initial stress of M for SV -wave on Energy coefficient E_3 versus θ_0 .

Figures 8 and 9 present the behaviour of amplitudes Z_1 and Z_2 for incident SV wave with respect the angle of incident θ_0 . The behaviour of Z_1 and Z_2 is similar with different magnitude values for all the cases of initial stress. From Fig.10, we examined that value of amplitude coefficient Z_3 increases smoothly for small values of θ_0 and decreases as the value of angle of incident (θ_0) increases for all values of initial stress under consideration i.e. 0.2, 0.4 and 0.6. Figures 11, 12 and 13 show the variation in the values of energy coefficients when SV wave is incident. The behaviour of E_1 , E_2 and E_3 is similar for incident SV wave as that of Z_1 , Z_2 and Z_3 for incident SV wave with difference in magnitude values.

4.2. Impact of gravity of medium M on reflection and energy coefficient for P and SV waves.

We examine the impact of gravity on variation of amplitude coefficient Z_1, Z_2, Z_3 and energy coefficients E_1, E_2 and E_3 with respect to angle of incident θ_0 for incident P and SV waves respectively. From figures 14, 15 and 16, the impact of gravity for longitudinal (P) wave on the reflection coefficients is

illustrated for different values of gravity i.e. for 0.2 , 0.4 and 0.6 w.r.t. angle of incidence θ_0 . Figure 14, it is observed that the behaviour of amplitude ratio Z_1 decreases smoothly for small values of θ_0 and increase gradually for remaining values of angle of incident. The value of Z_1 remain high for gravity value 0.6 . Figure 15 shows that Z_2 increases for small values of θ_0 up to 20° then decreases up to $\theta_0 = 38^\circ$ and becomes zero threat. Value of Z_2 increases very sharply for remaining values of angle of incident. From Fig.16, is noticed that the value of Z_3 decreases very sharply for small values of angle of incident and decrease gradually the after. Figures 17, 18 and 19 present the variation of energy coefficients E_1, E_2 and E_3 with respect to angle of incident for incident P wave under the impact of gravity. The behaviour of all energy coefficient E_1, E_2 and E_3 is almost similar to that of reflection coefficients Z_1, Z_2 , and Z_3 with difference in magnitude values for different values of angle of incident θ_0 when P wave is incident under the impact of gravity.

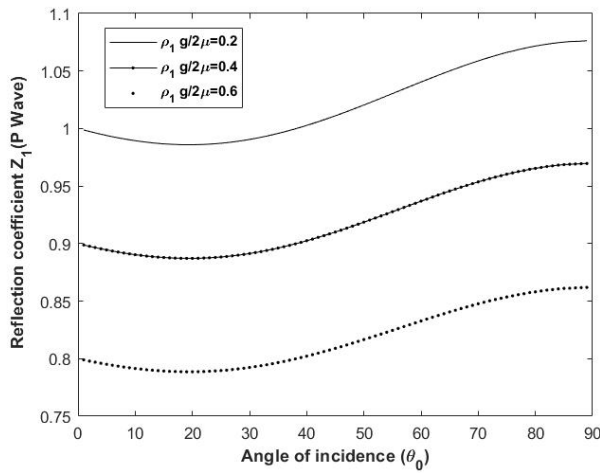


Fig.14. Impact of gravity of M for P -wave on Reflection coefficient Z_1 versus θ_0 .

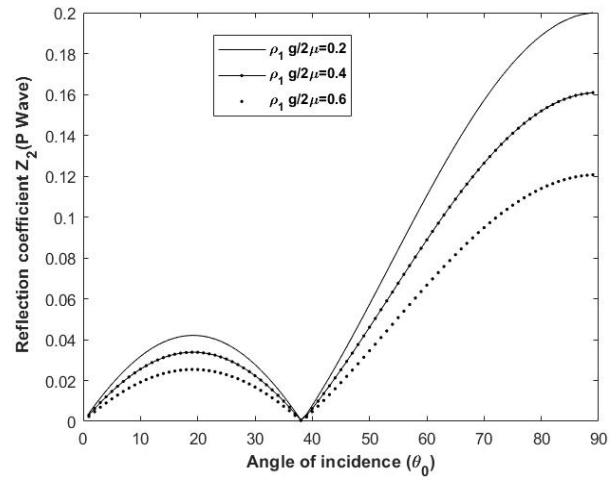


Fig.15. Impact of gravity of M for P -wave on Reflection coefficient Z_2 versus θ_0 .

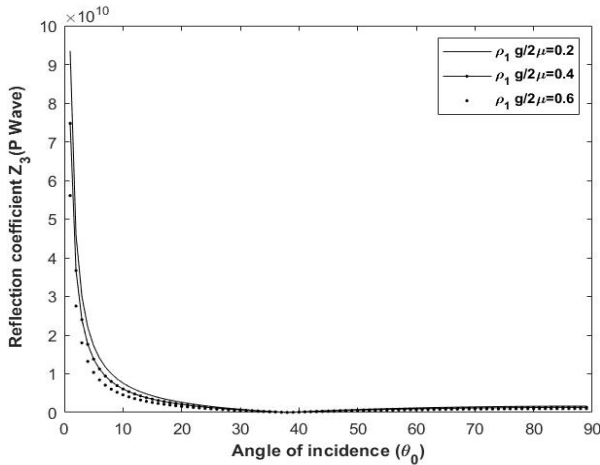


Fig.16. Impact of gravity of M for P -wave on Reflection coefficient Z_3 versus θ_0 .

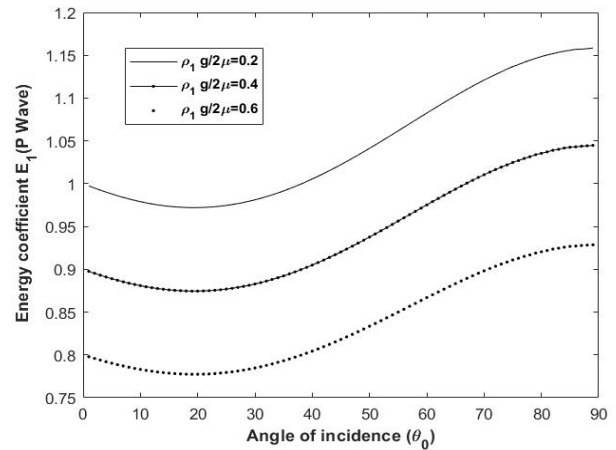


Fig.17. Impact of gravity of M for P -wave on Energy coefficient E_1 versus θ_0 .

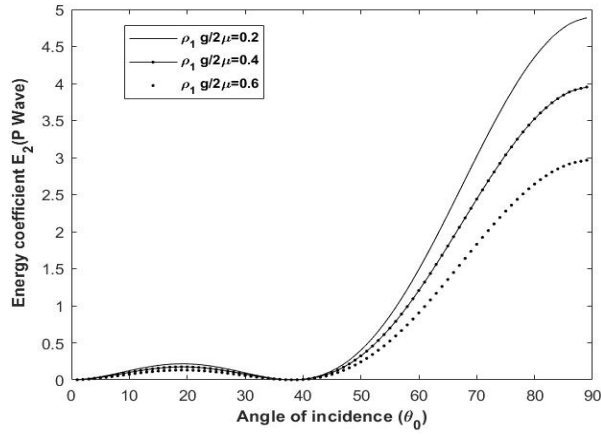


Fig.18. Impact of gravity of M for P -wave on Energy coefficient E_2 versus θ_0 .

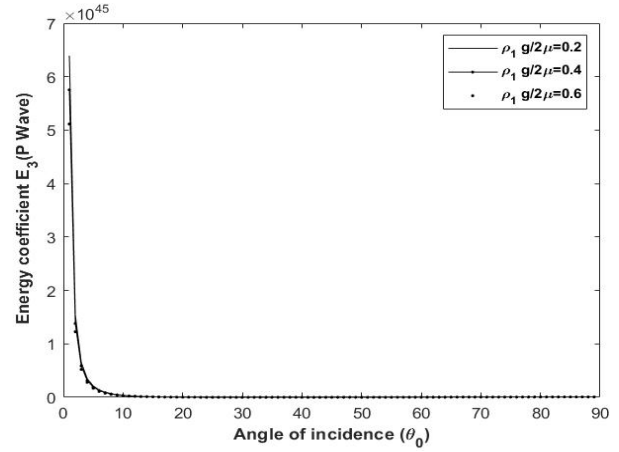


Fig.19. Impact of gravity of M for P -wave on Energy coefficient E_3 versus θ_0 .

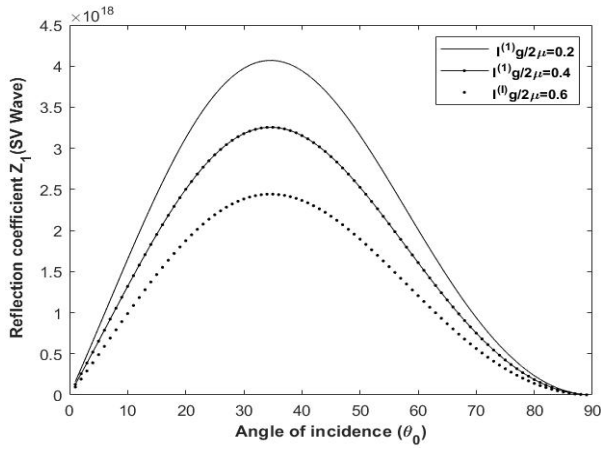


Fig.20. Impact of gravity of M for SV -wave on Reflection coefficient Z_1 versus θ_0 .

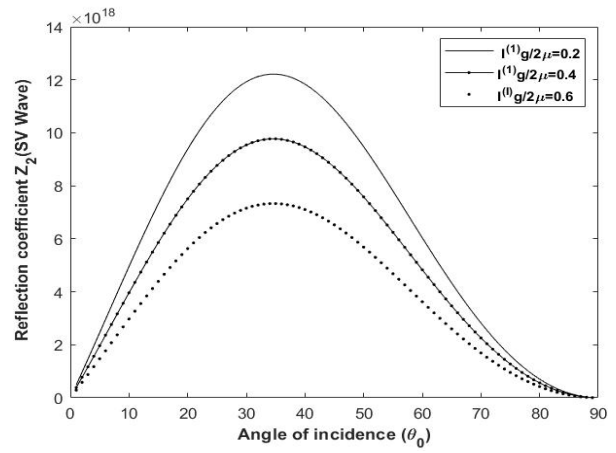


Fig.21. Impact of gravity of M for SV -wave on Reflection coefficient Z_2 versus θ_0 .

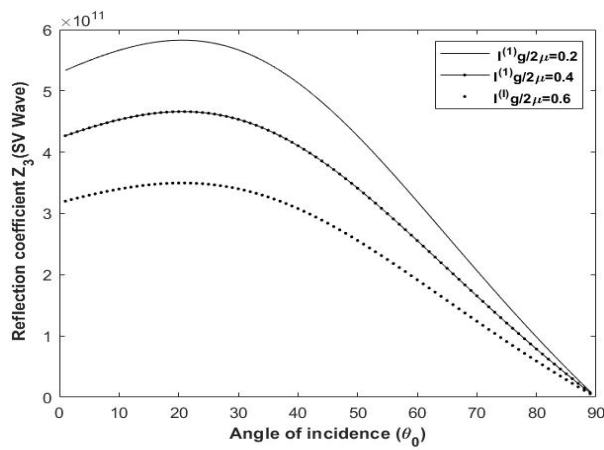


Fig.22. Impact of gravity of M for SV -wave on Reflection coefficient Z_3 versus θ_0 .

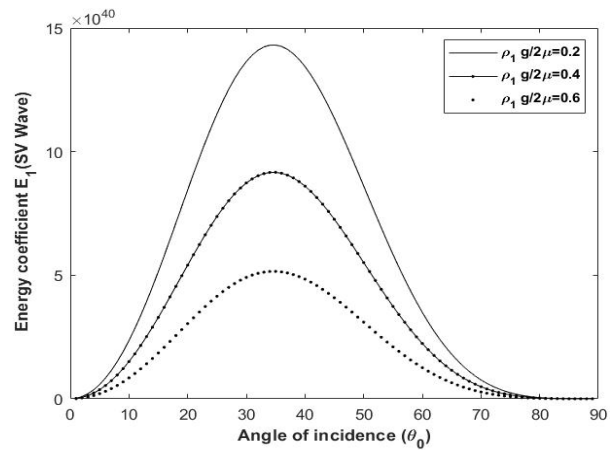


Fig.23. Impact of gravity of M for SV -wave on Energy coefficient E_4 versus θ_0 .

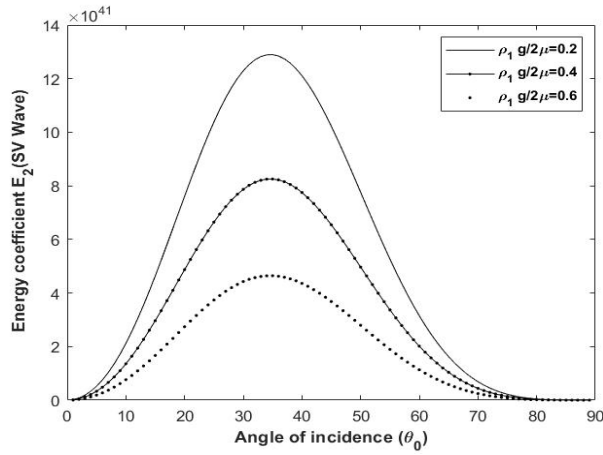


Fig.24. Impact of gravity of M for SV -wave on Energy coefficient E_2 versus θ_0 .

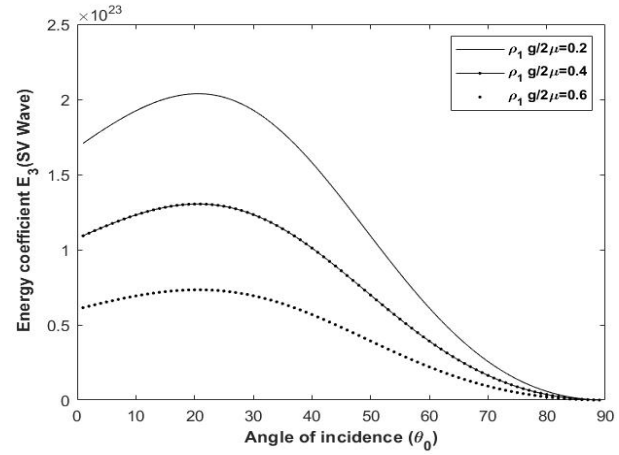


Fig.25. Impact of gravity of M for SV -wave on Energy coefficient E_3 versus θ_0 .

Figures 19, 20 and 21 reflect the behaviour of amplitude coefficients Z_1, Z_2 , and Z_3 whereas the behaviour of energy coefficient E_1, E_2 and E_3 is presented by Figs 22, 23 and 24 for incident SV wave under the influence of gravity. Figures 19 and 20 show that the value of Z_1 and Z_2 increase sharply as the value of angle of incident θ_0 increases up to $\theta_0 = 35^\circ$ and decrease sharply thereafter and becomes 0 at $\theta_0 = 90^\circ$. Similar behaviour of energy coefficient E_1, E_2 is observed from Figs 22 and 23. From Figs 21, 24 it is noticed that reflection coefficient Z_3 and energy coefficient E_3 increase gradually for small values of angle of incident θ_0 and decrease fastly as angle of incident increases.

5. Conclusion

From this paper, it is noticed that:

- 1) under the impact of initial stress, Z_1 and E_1 trends are nearly identical for incident P and SV waves for all values.
- 2) Z_2 and E_2 for incident P waves exhibit opposite behaviour to that of incident SV waves. Additionally, it is observed that when initial stress is taken into account, the value of E_1 for incident P waves decreases more abruptly than Z_1 .
- 3) due to the impact of initial stress, values of Z_3 and E_3 decrease sharply for small range of θ_0 and decrease smoothly for higher values of incident angles for incident P wave whereas values of Z_3 and E_3 increase for smaller of incident angles and decrease gradually for higher values of θ_0 in case of incident SV wave.
- 4) trends are similar for Z_1 and E_1 when gravity is taken into account and oscillating behaviour is noticed for smaller values of incident angles and increase sharply after $\theta_0 > 38^\circ$ for Z_2 and E_2 for incident P wave.
- 5) decreasing behaviour is observed for Z_3 and E_3 for incident P wave in case of gravity.
- 6) trends for Z_1, Z_2, Z_3 are similar to that of E_1, E_2, E_3 for incident SV wave with impact of gravity.

Nomenclature

E_1, E_2, E_3 – energy coefficients

h_l – pressure

$I_{xx}^{(l)}, I_{zz}^{(l)}$ – initial stresses

l – wave number

S – velocity

Z_1, Z_2, Z_3 – amplitude ratios

ρ_l – density

ϕ – displacement potential

ψ – displacement potential

References

- [1] Biot M.A. (1940): *The influence of initial stress on elastic waves.*– J. Appl. Phys., vol.11, No.9, pp.522-530, <https://doi.org/10.1063/1.1712807>.
- [2] Edelen D.G.B. and Laws N. (1971): *On the thermodynamics of systems with nonlocality.*– Arch. Rational Mech. Anal., vol.43, No.1, pp.24-35. <https://doi.org/10.1007/BF00251543>.
- [3] Edelen D.G.B., Green A.E. and Laws N. (1971): *Nonlocal continuum mechanics.*– Arch. Rational Mech. Anal., vol.43, No.1, pp.36-44, <https://doi.org/10.1007/BF00251544>.
- [4] Eringen A.C. and Edelen D.G.B. (1972): *On nonlocal elasticity.*– Int. J. Eng. Sci., vol.10, No.3, pp.233-248, [https://doi.org/10.1016/0020-7225\(72\)90039-0](https://doi.org/10.1016/0020-7225(72)90039-0).
- [5] Altan S.B. (1989): *Uniqueness of initial-boundary value problems in nonlocal elasticity.*– Int. J. of Solids and Structures, vol.25, No.11, pp.1271-1278, [https://doi.org/10.1016/0020-7683\(89\)90091-7](https://doi.org/10.1016/0020-7683(89)90091-7).
- [6] Othman M.I. and Song Y. (2007): *Reflection of plane waves from an elastic solid half-spaces under hydrostatic initial stress without energy dissipation.*– Int. J. Solids Struct., vol.44, No.17, pp.5651-5664, <https://doi.org/10.1016/j.ijsolstr.2007.01.022>.
- [7] Abd-Alla A.N. and Al-Sheikh F.A. (2009): *The effect of the initial stresses on the reflection and transmission of plane quasi-vertical transverse waves in piezoelectric materials.*– World Acad. Sci. Eng. Tech., vol.3, No.2, pp.118-125.
- [8] Abd-Alla A.M., Abo-Dahab S.M. and Al-Thamali T.A. (2012): *Propagation of Rayleigh waves in a rotating orthotropic material elastic half-space under initial stress and gravity.*– J Mech Sci Tech., vol. 26, pp.2815-2823, <https://doi.org/10.1007/s12206-012-0736-5>.
- [9] Guo X. and Wei P.(2014): *Effects of initial stress on the reflection and transmission waves at the interface between two piezoelectric half-spaces.*– Int. J. Solids Struct., vol.51, No.21-22, pp.3735-3751, <https://doi.org/10.1016/j.ijsolstr.2014.07.008>.
- [10] Othman M.I.A., Abo-Dahab S.M. and Alsebaey O.N.S. (2017): *Reflection of plane waves from a rotating magnetothermoelastic medium with two temperature and initial stress under three theories.*– Mech. Eng., vol.21, No.2, pp.217-232.
- [11] Das N., Sarkar N. and Lahiri A. (2019): *Reflection of plane waves from the stress-free isothermal and insulated boundaries of a nonlocal thermoelastic solid.*– Applied Mathematical Modelling, vol.73, pp.526-542, <https://doi.org/10.1016/j.apm.2019.04.028>.
- [12] Tothhawang L. and Singh S.S. (2020): *Effect of initial stresses on the elastic waves in transversely isotropic thermoelastic materials.*– Wiley, pp.1-14, <https://doi.org/10.1002/eng2.12104>.
- [13] Poonam, Sahrawat R. K., Kumar K. and Arti (2021): *Plane wave propagation in functionally graded isotropic couple stress thermoelastic solid media under initial stress and gravity.*– Eur. Phys. J. Plus, vol.136, No.114, <https://doi.org/10.1140/epjp/s13360-021-01097-5>.

- [14] Day S., Gupta A.K. and Gupta S. (2002): *Effect of gravity and initial stress on torsional surface waves in dry sandy medium.*– Journal of Engineering Mechanics, vol.128, No.10, pp.1115-1118, DOI:10.1061/(ASCE)0733-9399(2002)128:10(1116).
- [15] Biot M.A. (1965): *Mechanics of Incremental Deformations.*– Wiley, New York.
- [16] Szekeres A. (1980): *Equation system of thermoelasticity using the modified law of thermal conductivity.*– Periodica Polytechnica Mech. Eng., vol.24, No.3, pp.253-261.
- [17] Farkas I. and Szekeres A. (1984): *Application of the modified law of heat conduction and state equation to dynamical problems of thermoelasticity.*– Periodica Polytechnica Mech. Eng., vol.28, No.2-3, pp.163-170.
- [18] Chandrasekhariah D.S. (1998): *Hyperbolic thermoelasticity: A review of recent literature.*– Appl. Mech. Rev., vol.51, No.12, pp.705-729, <http://dx.doi.org/10.1115/1.3098984>.
- [19] Lord H.W. and Shulman Y. (1967): *A generalized dynamical theory of thermoelasticity.*– J. Mech. Phys. Solid., vol.15, No.5, pp.299-309, [http://dx.doi.org/10.1016/0022-5096\(67\)90024-5](http://dx.doi.org/10.1016/0022-5096(67)90024-5).
- [20] Green A.E. and Lindsay A. (1972): *Thermoelasticity.*– J. Elasticity, vol.2, pp.1-7, <https://doi.org/10.1007/BF00045689>.
- [21] Hetnarski R.B. and Ignaczak J. (1999): *Generalized thermoelasticity.*– J. Therm. Stresses, vol.22, No.4-5, pp.451-476, doi:10.1080/014957399280832.
- [22] Green A.E. and Naghdi P.M. (1993): *Thermoelasticity without energy dissipation.*– J. Elasticity, vol.31, pp.189-208, <https://doi.org/10.1007/BF00044969>.
- [23] Tzou D.Y. (1995): *A unified approach for heat conduction from macro to micro-scales.*– J. Heat Trans., vol.117, No.1, pp.8-16, <https://doi.org/10.1115/1.2822329>.
- [24] Inan E. and Eringen A.C. (1991): *Nonlocal theory of wave propagation in thermoelastic plates.*– Int. J. Engng. Sci., vol.29, No.7, pp.831-843, [https://doi.org/10.1016/0020-7225\(91\)90005-N](https://doi.org/10.1016/0020-7225(91)90005-N).
- [25] Eringen A.C. (2002): *Non-Local Continuum Field Theories.*– Springer-Verlag, New York, <https://doi.org/10.1007/b97697>.
- [26] Khurana A. and Tomar S.K. (2016): *Wave propagation in nonlocal microstretch solid.*– Applied Mathematical Modelling, vol.40, No.11-12, pp.5858-5875, <https://doi.org/10.1016/j.apm.2016.01.035>.
- [27] Kumar R. and Kumar K. (2016): *Reflection and transmission at the boundary surface of modified couple stress thermoelastic media.*– Int. J. of Applied Mechanics and Engineering, vol.21, No.1, pp.61-81, <https://doi.org/10.1515/ijame-2016-0004>.
- [28] Singh D., Kaur G. and Tomar S.K., (2017): *Waves in nonlocal elastic solid with voids.*– Journal of Elasticity, vol.128, pp.85-114, <https://doi.org/10.1007/s10659-016-9618-x>.
- [29] Kaur G., Singh D. and Tomar S. K. (2018): *Rayleigh-type wave in a nonlocal elastic solid with voids.*– European Journal of Mechanics-/A Solids, vol.71, pp.134-150, <https://doi.org/10.1016/j.euromechsol.2018.03.015>.
- [30] Sarkar N. and Tomar S.K. (2019): *Plane waves in nonlocal thermoelastic solid with voids.*– Journal of Thermal Stresses, vol.42, No.5, pp.580-606, <https://doi.org/10.1080/01495739.2018.1554395>.
- [31] Sahrawat K., Poonam and Kumar K. (2020): *Wave propagation in nonlocal couple stress thermoelastic solid.*– AIP Conference Proceedings, vol.2253, No.1, pp.20-26, <https://doi.org/10.1063/5.0018979>.
- [32] Pramanik A.S. and Biswas S. (2020): *Surface waves in non-local thermoelastic medium with state space approach.*– Journal of Thermal Stress, vol.43, No.6, pp.667-686, <https://doi.org/10.1080/01495739.2020.1734129>.
- [33] Poonam, Sahrawat R.K. and Kumar K. (2021): *Plane wave propagation and fundamental solution in non-local couple stress micropolar thermoelastic solid medium with voids.*– Waves in Random and Complex Media, vol.34, No.2, pp.879-914, <https://doi.org/10.1080/17455030.2021.1921312>.
- [34] Gupta D., Malik S., Kumar K. and Sharma R.K. (2022): *Reflection and transmission in non-local couple stress micropolar thermoelastic media.*– Int. J. of Appl. Mech. and Engg., vol.27, No.2, pp.53-76, <https://doi.org/10.2478/ijame-2022-0019>.
- [35] Balta. F and Suhubi E.S. (1977): *Theory of nonlocal generalized thermoelasticity.*– International Journal of Engineering Science, vol.15, No.9-10, pp.579-588, [https://doi.org/10.1016/0020-7225\(77\)90054-4](https://doi.org/10.1016/0020-7225(77)90054-4).
- [36] Ali H., Bibi F., Azhar E. and Jamal M. (2023): *Analyzing Hall current effects and fractional order nonlocal theory on plane wave reflection in a rotating isotropic medium.*– International Journal of Computational Materials Science and Engineering, vol.14, No.2, <https://doi.org/10.1142/S2047684123500501>.
- [37] Bibi F., Ali H., Azhar E., Jamal M., Ahmed I. and Ragab A.E. (2023): *Propagation and reflection of thermoelastic wave in a rotating nonlocal fractional order porous medium under Hall current influence.*– Scientific Reports, vol.13, No.17703, <https://doi.org/10.1038/s41598-023-44712-4>.

- [38] Azhar E., Bibi F., Ali H. and Jamal M. (2024): *Influence of Hall current on thermoelastic wave behavior in viscoelastic fractional-order rotating porous solids.*– Arabian Journal for Science and Engineering, vol.49, No.12, pp.9947-9965, <https://doi.org/10.1007/s13369-024-08704-4>.
- [39] Azhar E., Bibi F., Ali H. and Jamal M. (2024): *Investigating reflection phenomenon of plane waves in a fractional order thermoelastic rotating medium using nonlocal theory.*– Mechanics of Time-Dependent Materials, vol.28, No.3, pp.1375-1393, <https://doi.org/10.1007/s11043-024-09709-0>.
- [40] Bibi F and Ali H. (2024): *Reflection and transmission phenomenon of plane waves at the interface of diffusive viscoelastic porous rotating isotropic medium under hall current and nonlocal thermoelastic porous solid.*– The Journal of Strain Analysis for Engineering Design, vol.59, No.7, pp.491-516, <https://doi.org/10.1177/03093247241259818>.
- [41] Singh B. and Bijarnia R. (2021): *Non local effects on propagation of waves in a generalized thermoelastic solid half space.*– Structural Engineering and Mechanics, vol.77, No.4, pp.473-479, <https://doi.org/10.12989/sem.2021.77.4.473>.

Received: February 28, 2025

Revised: September 10, 2025